

# Sphingosine 1-Phosphate Reduces Vascular Leak in Murine and Canine Models of Acute Lung Injury

Bryan J. McVerry, Xinqi Peng, Paul M. Hassoun, Saad Sammani, Brett A. Simon, and Joe G. N. Garcia

Division of Pulmonary and Critical Care Medicine and Division of Pulmonary and Critical Care Medicine, Center for Translational Respiratory Medicine, Johns Hopkins University School of Medicine, Baltimore, Maryland

Excessive mechanical stress is a key component of ventilator-associated lung injury, resulting in profound vascular leak and an intense inflammatory response. To extend our *in vitro* observations concerning the barrier-protective effects of the lipid growth factor sphingosine 1-phosphate (Sph 1-P), we assessed the ability of Sph 1-P to prevent regional pulmonary edema accumulation in clinically relevant rodent and canine models of acute lung injury induced by combined intrabronchial endotoxin administration and high tidal volume mechanical ventilation. Intravenously delivered Sph 1-P significantly attenuated both alveolar and vascular barrier dysfunction while significantly reducing shunt formation associated with lung injury. Whole lung computed tomographic image analysis demonstrated the capability of Sph 1-P to abrogate significantly the accumulation of extravascular lung water evoked by 6-hour exposure to endotoxin. Axial density profiles and vertical density gradients localized the Sph 1-P response to transitional zones between aerated and consolidated lung regions. Together, these results indicate that Sph 1-P represents a novel therapeutic intervention for the prevention of pulmonary edema related to inflammatory injury and increased vascular permeability.

**Keywords:** acute lung injury; computed tomography imaging; endothelial permeability; mechanical ventilation

The key pathophysiologic feature of acute lung injury (ALI) and ventilator-associated lung injury is a sustained duration of high-permeability lung edema, which in addition to producing physiologic derangement (hypoxemia and reduced lung compliance) increases the need for and duration of ventilatory support. It is now appreciated that increased requirements for mechanical ventilation enhance the risk of malnutrition, nosocomial infection, and multiple organ dysfunction syndrome. Clearly, therapies aimed at minimizing the vascular leak underlying ALI will decrease the duration of mechanical ventilation and may have substantial impact on morbidity and mortality associated with ALI. Effective adjunctive therapies to treat or prevent ALI or ventilator-associated lung injury, however, remain elusive (1–5).

Platelets have long been demonstrated to enhance the integrity of the microcirculation (6, 7) with thrombocytopenia increasing capillary permeability and accelerating fluid and protein extravasation (8, 9). Infusion of platelets or platelet-released products reverses the barrier compromise seen in thrombocytopenia (10). Recently, we identified sphingosine 1-phosphate (Sph

1-P), a biologically active lipid generated by hydrolysis of membrane lipids primarily in activated platelets, as the major barrier-protective product of platelets (11, 12). Through ligation of cell surface endothelial differentiation gene receptors, Sph 1-P initiates downstream cytoskeletal reorganization, resulting in improved endothelial barrier function *in vitro* (12). We recently translated these *in vitro* observations into an *in vivo* model of sepsis/ALI in which C57BL/6 mice exposed to intratracheal lipopolysaccharide (LPS) (2 mg/kg) followed by intravenous Sph 1-P (1  $\mu$ M) demonstrated reduced lung wet-weight to dry-weight ratios, decreased extravasation of Evans blue dye into the pulmonary interstitium, and attenuated accumulation of alveolar protein after 6 and 24 hours compared with mice exposed to intratracheal LPS alone (13). Although rodent models provide an efficient means to establish the therapeutic potential of barrier-protective approaches, they do not allow for evaluation of regional differences in lung mechanical and cellular behavior now well recognized as characteristic of ALI in humans (14, 15). Therefore, large animal experiments in injury models with appropriate scale and mechanical characteristics are essential to the translation of these therapies into the practice of critical care medicine. As vascular barrier-protective strategies for the treatment of ALI are not currently available, we hypothesized that Sph 1-P-induced endothelial barrier enhancement would attenuate lung edema formation in a rodent model of pure ventilator-induced lung injury as well as decrease regional vascular leak in a clinically relevant canine model of LPS-induced, ventilator-associated ALI. Our results strongly support further consideration of Sph 1-P as a novel therapeutic intervention for ALI. Some of the results of these studies have been previously published in abstract form (16, 17).

## METHODS

Johns Hopkins University Institutional Animal Care and Use Committee approved all animal protocols. Additional method details are reported in the online supplement.

### Mouse Ventilator-induced Lung Injury Preparation

C57BL/6 mice were anesthetized and tracheostomized, and the jugular vein was cannulated. Mice were treated with intravenous saline or Sph 1-P (Sigma Co., St. Louis, MO) and 2 hours of high- $V_T$  (17 cc/kg) mechanical ventilation. Lung capillary leakage in mice was assessed using Evans blue dye extravasation as we previously described (13).

### Canine ALI Preparation

Twenty-one male beagles (13–18 kg) were anesthetized with pentobarbital and pancuronium. Tracheostomy, femoral artery and vein cannulation, and pulmonary artery catheter placement were performed. Volume-controlled mechanical ventilation (Lifecare PLV-102) was initiated with high- $V_T$  (17 cc/kg), positive end-expiratory pressure (5 cm H<sub>2</sub>O), and the rate was set to achieve an end-tidal (partial) carbon dioxide pressure ( $P_{ETCO_2}$ ) of 30–35 mm Hg and subsequently adjusted to maintain pH of more than 7.20.  $F_{IO_2}$  of 0.30 was increased as required to maintain  $Sa_{O_2}$  of more than 88% or  $Pa_{O_2}$  of more than 60 mm Hg. Recruitment sighs of three times  $V_T$  were performed hourly. Airway, arterial, pulmonary artery, and central venous pressures,  $Sa_{O_2}$ , and  $P_{ETCO_2}$  were monitored continuously. Serial measurement of arterial and mixed venous blood gases quantified gas exchange. Venous admix-

(Received in original form May 28, 2004; accepted in final form July 23, 2004)

Supported by NIH/NHLBI T32 HL07534, NIH/NHLBI F32 HL74569, NIH/NHLBI HL58064, NIH HL64368, NIH/NHLBI HL049441, and SCCOR P50 HL073994.

Correspondence and requests for reprints should be addressed to Joe G. N. Garcia, M.D., Johns Hopkins University School of Medicine, Division of Pulmonary and Critical Care Medicine, 1830 East Monument Street Room 527, Baltimore, MD 21287. E-mail: drgarcia@jhmi.edu

This article has an online supplement, which is accessible from this issue's table of contents online at [www.atsjournals.org](http://www.atsjournals.org)

Am J Respir Crit Care Med Vol 170, pp 987–993, 2004

Originally Published in Press as DOI: 10.1164/rccm.200405-684OC on July 28, 2004

Internet address: [www.atsjournals.org](http://www.atsjournals.org)

ture ( $Q_s/Q_t$ ) was calculated using standard equations (18). All previously mentioned parameters plus pulmonary artery occlusion pressure and cardiac output were recorded hourly. Intravenous saline was administered continuously and bolused as needed for hypotension or for hemoconcentration per protocol. Animals were killed at the conclusion of the study with supplemental pentobarbital followed by exsanguination.

### Endotoxin and Sph 1-P Delivery

*Escherichia coli* LPS (O55:B5 Sigma L4005), 2 mg/kg, was delivered intrabronchially through an 18-gauge catheter introduced into each of five lobar bronchi via the working channel of a fiberoptic bronchoscope (Olympus, Melville, NY). Nine beagles received Sph 1-P (85  $\mu$ g/kg; Sigma Co.) via a 20-minute infusion concomitant with LPS instillation.

### Bronchoalveolar Lavage Protein Concentration

Bilateral bronchoalveolar lavage was performed with 20-cc aliquots of saline for serial determination of bronchoalveolar lavage fluid protein concentration.

### Computed Tomography

Six dogs were studied 6 hours after injury induction using contiguous 1-mm computed tomographic (CT) (Aquilion 16, Toshiba, New York, NY) images spanning the lung from apex to base obtained in the supine position. Images were gated at end inspiration and end expiration during steady-state mechanical ventilation, two four-slice image acquisitions per breath, with 2-mm incremental table movement between acquisitions. The lung tissue in each slice was segmented from the chest wall and mediastinum and analyzed using PASS image analysis software (University of Iowa Division of Physiological Imaging, Iowa City, IA). Whole lung total, air, and tissue volumes, axial density profiles, and vertical density profiles were generated as global and regional measures of injury severity (15, 19–21).

### Statistical Analysis

Venous admixture at each time point and CT data were compared using the Student's paired *t* test. Linear regression was performed to compare oxygenation trends beyond 90 minutes. Bronchoalveolar lavage protein accumulation within groups was analyzed using a one-way analysis of variance with repeated measures and between groups using two-way analysis of variance. Data are presented as mean  $\pm$  SEM with statistical significance defined at  $p < 0.05$ .

## RESULTS

### Murine Physiologic Assessment

C57BL/6 mice were injured by a 2-hour exposure to high- $V_T$  mechanical ventilation (17 cc/kg). Mice were infused with either normal saline or Sph 1-P (1  $\mu$ M) 1 hour after initiation of mechanical ventilation ( $n = 4$  each group). Lungs were harvested and assayed for vascular leak quantified by lung tissue homogenate Evans blue dye concentration standardized to body weight (Figure 1). Mechanical ventilation directly increased tissue Evans blue concentration (> 80% increase) compared with control mice ( $0.129 \pm 0.014$  vs.  $0.071 \pm 0.005$   $\mu$ g/ml  $g^{-1}$ , mean  $\pm$  SEM,  $p = 0.002$ ). Sph 1-P infusion after initiation of mechanical ventilation attenuated Evans blue extravasation (> 30% inhibition) compared with ventilation alone ( $0.090 \pm 0.009$  vs.  $0.129 \pm 0.014$   $\mu$ g/ml  $g^{-1}$ ,  $p = 0.04$ ), achieving levels similar to control mice ( $0.09 \pm 0.009$  vs.  $0.071 \pm 0.005$   $\mu$ g/ml  $g^{-1}$ ,  $p = 0.07$ ).

### Canine Global Physiologic Assessment

Beagles were injured with intrabronchial LPS ( $n = 21$ ), with one group of animals concomitantly infused with Sph 1-P ( $n = 9$ ). Intrabronchial LPS administration (2 mg/kg) resulted in the development of severe lung injury with rapid increases in  $Q_s/Q_t$  immediately after LPS instillation, progressing over the duration of the support period ( $5.8 \pm 3.4\%$  to  $41.72 \pm 3.9\%$  after 8 hours) (Figure 2). In conjunction with the increase in  $Q_s/Q_t$ , bronchoalveolar lavage protein progressively increased after

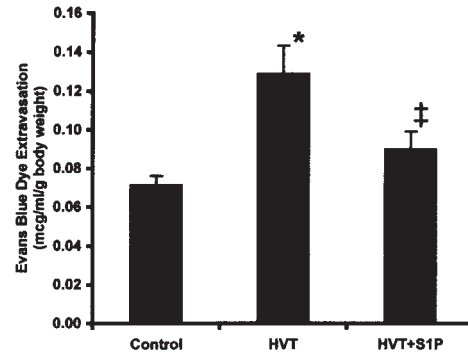


**Figure 1.** Intravenous sphingosine 1-phosphate (Sph 1-P) attenuates vascular leak in a murine model of high- $V_T$  mechanical ventilation-induced permeability. Shown are the levels of extravasated Evans blue dye ( $\mu$ g/ml/g body weight) in mouse lung homogenate sampled from spontaneously ventilating C57BL/6 mice (control,  $n = 5$ ), high- $V_T$  mechanically ventilated mice (HVT,  $V_T = 17$  cc/kg, 2 hours,  $n = 4$ ), and mechanically ventilated mice that received intravenous Sph 1-P (1  $\mu$ M) 1 hour after the onset of mechanical ventilation (HVT + S1P,  $V_T = 17$  cc/kg,  $n = 4$ ). \* $p < 0.05$  compared with control; † $p < 0.05$  compared with HVT.

LPS injury with 6 hours of ventilation (5.2-fold increase over baseline; Figure 3).

### CT Quantification of Injury

Lung tissue volume measurements obtained by CT, which include vascular structures, airway structures, lung parenchyma, and extravascular lung water, account for approximately 30% ( $28.0 \pm 2.9\%$ ) of the total lung volume at 5-cm  $H_2O$  positive end-expiratory pressure in the uninjured canine lung (Figure 4). Assuming a constant pulmonary blood volume, an increase in lung tissue volume after injury reflects lung water accumulation (15, 22). In well established canine models of lung injury

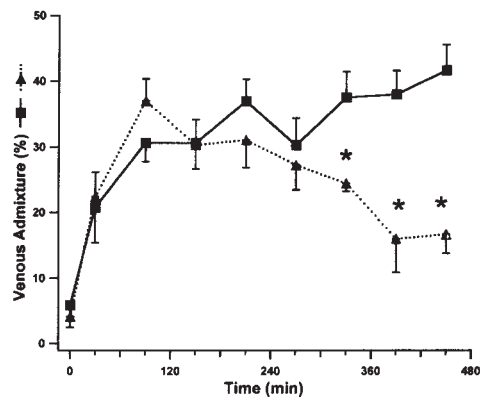


**Figure 2.** Intravenous Sph 1-P attenuates lipopolysaccharide (LPS)-induced shunt formation in a canine model of ventilator-associated lung injury. Depicted is the time course of venous admixture formation in anesthetized beagles subjected to high- $V_T$  mechanical ventilation (17 cc/kg) after treatment with intrabronchial LPS (2 mg/kg, black squares,  $n = 12$ ) or intrabronchial LPS plus concomitant intravenous Sph 1-P (85  $\mu$ g/kg, dotted line, triangles,  $n = 9$ ). Beagles receiving intravenous Sph 1-P demonstrated significant reductions in shunt formation beginning 5.5 hours after exposure to LPS compared with dogs receiving LPS alone. After 5.5 hours,  $n = 3$ . Mean  $\pm$  SEM. \* $p \leq 0.05$ .

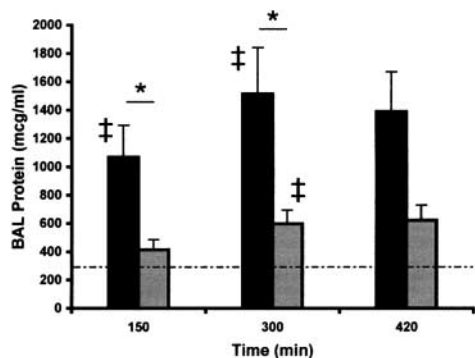


**Figure 3.** Intravenous Sph 1-P attenuates LPS-induced bronchoalveolar lavage (BAL) protein accumulation in a canine model of ventilator-associated lung injury. Shown is the time course of BAL fluid protein accumulation in anesthetized beagles subjected to high-V<sub>T</sub> mechanical ventilation (17 cc/kg) after treatment with intrabronchial LPS (2 mg/kg, black bars, n = 10) or intrabronchial LPS plus concomitant intravenous Sph-1-P (85 µg/kg, gray bars, n = 7). Baseline BAL protein concentration was 279 ± 45.2 µg/ml (dashed line). After 6 hours, n = 3. Mean ± SEM. \*p ≤ 0.05; ‡p < 0.05 compared with baseline.

(oleic acid and saline lavage) with worse degrees of hypoxemia, lung tissue density increased approximately 1.4-fold after injury (39.1 ± 7.97% and 43.9 ± 6.9% respectively; Figure 4) compared with control dogs (23, 24). In our endotoxin model, LPS induced a 1.7-fold increase in lung tissue volume compared with historic control subjects (48.6 ± 5.71% vs. 28.0 ± 2.9%; Figures 4 and 5).

**Effect of Sph 1-P on Canine Ventilator-associated Lung Injury**

After an initial rise in Q<sub>e</sub>/Q<sub>t</sub> similar to that observed in the LPS control group, intravenously delivered Sph 1-P attenuated any further impairment in oxygenation with significant improve-

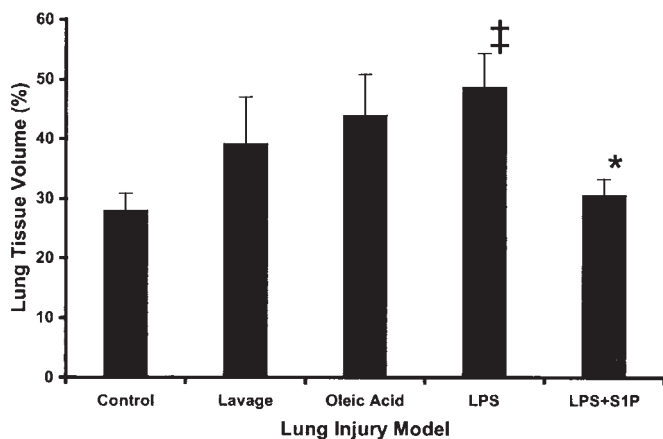


**Figure 4.** Intravenous Sph 1-P abrogates computed tomographic (CT) evidence for LPS-induced lung water accumulation in a canine model of ventilator-associated lung injury. Shown is CT quantification of end-expiratory lung tissue volume in normal dogs (n = 8), dogs injured with oleic acid (0.08 ml/kg intravenously over 20 minutes, n = 4), dogs injured with large volume warmed saline lavage (60 cc repeated every 10 minutes until Pa<sub>o2</sub> < 90 mm Hg, n = 4) (24), dogs injured with intrabronchial LPS (2 mg/kg, n = 3), and dogs injured with LPS (2 mg/kg) and treated concomitantly with intravenous Sph 1-P (85 mcg/kg, n = 3). All animals were imaged at positive end-expiratory pressure (5 cm H<sub>2</sub>O). \*p < 0.05 compared with LPS; ‡p < 0.05 compared with control.

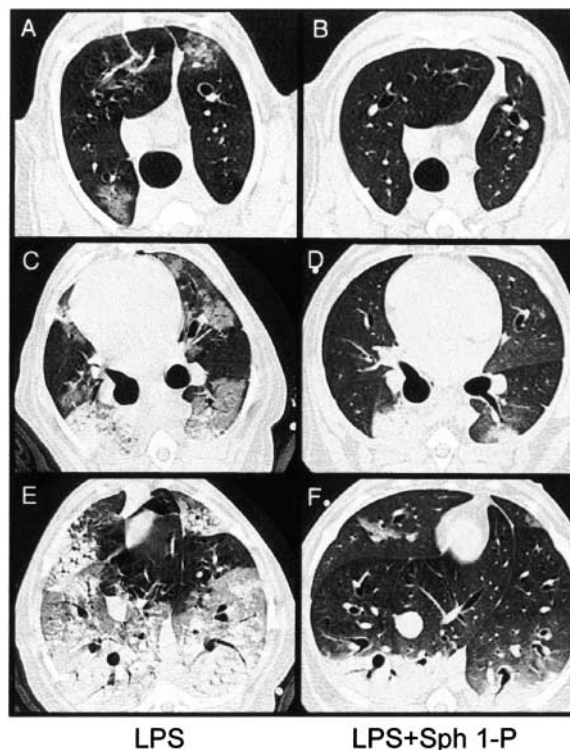


**Figure 5.** Intravenous Sph 1-P attenuates pulmonary edema formation in response to LPS in a canine model of ventilator-associated lung injury. Depicted are CT images of beagle lungs after 6 hours of high-V<sub>T</sub> mechanical ventilation (17 cc/kg) after injury with intrabronchial LPS (2 mg/kg, A, C, E) or intrabronchial LPS plus concomitant treatment with iv Sph 1-P (85 µg/kg, B, D, F). Sections represent similar regions from apical (A and B), infracarinal (C and D), and basilar (E and F) regions of each animal. Sph 1-P grossly attenuates regional lung injury in LPS-injured lungs. Images are not to scale.

ments seen after 5 hours (p < 0.05) (Figure 2). By the completion of the observation period, Q<sub>e</sub>/Q<sub>t</sub> had declined from a peak of 37.0 ± 3.34% to 16.7 ± 2.85%, a striking improvement (approximately 55%) compared with LPS-treated animals, which did not receive Sph 1-P. Corresponding to the improvement in shunt formation, the increase in bronchoalveolar lavage protein induced by LPS was largely abrogated by the infusion of Sph 1-P in LPS-challenged dogs (p < 0.05) (Figure 3), with a more than 60% decrease in Sph 1-P-treated animals after 6 hours. By CT analysis, Sph 1-P attenuated the accumulation of lung water induced by LPS (tissue volume [% total] 30.5 ± 2.7% LPS + Sph 1-P vs. 48.6 ± 5.7% LPS alone) to a level comparable to normal historic control animals (p = 0.49) (Figures 4 and 5).

**Effect of Sph 1-P on Canine Regional Physiologic Derangement**

As previously stated, the advantage of the large animal model is the regional information provided. End-inspiratory CT images in this LPS/ventilator-associated lung injury model demonstrates bilateral heterogeneous infiltrates involving all lung regions in animals injured with intratracheal LPS (Figure 5). Consistent with a vascular barrier protective action, regional edema accumulation is markedly diminished in dogs treated concomitantly with intravenous Sph 1-P (Figure 5). Craniocaudal (axial) volume profiles at end-expiration demonstrate increased air volume and decreased density throughout the lungs, particularly in mid-

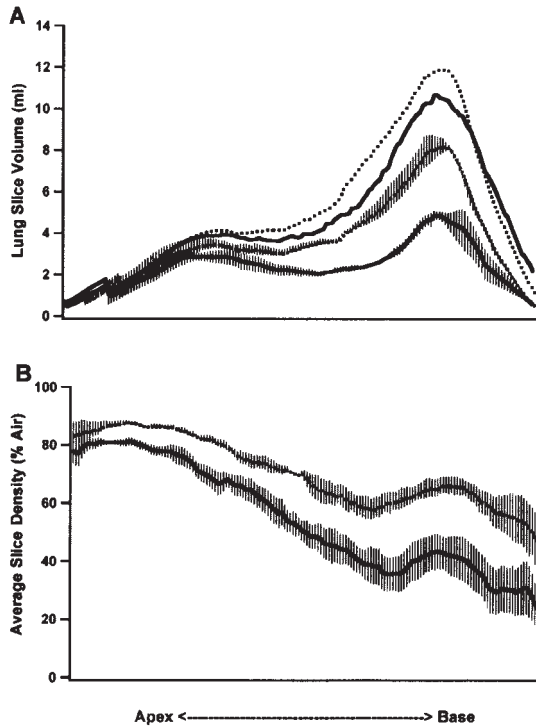


**Figure 6.** Intravenous Sph 1-P improves basilar aeration after intrabronchial LPS instillation in a canine model of ventilator-associated lung injury. (A) Craniocaudal (axial) end-expiratory volume profiles of mechanically ventilated beagles 6 hours after LPS instillation (solid line, total volume; solid line with error bars, air volume,  $n = 3$ ) and after LPS instillation with concomitant Sph 1-P (dotted line, total volume; dotted line with error bars, air volume,  $n = 3$ ). (B) CT generated whole-lung axial tissue density profiles of anesthetized beagles after 6 hours of high- $V_T$  (17 cc/kg) mechanical ventilation after treatment with intrabronchial LPS (2 mg/kg, solid,  $n = 3$ ) or intrabronchial LPS plus concomitant intravenous Sph 1-P (85  $\mu$ g/kg, dotted,  $n = 3$ ); 0 Hounsfield units (HU) corresponds to 100% tissue density, whereas -1,000 Hounsfield Units corresponds to 100% air. Sph 1-P markedly attenuates edema formation after LPS represented by the increased air content in all lung regions inferior to the apical zones. Data represent mean  $\pm$  SEM after standardization of lung size.

lung and basilar regions of dogs treated with Sph 1-P after LPS instillation compared with LPS instillation alone (Figure 6A). Vertical density gradients quantifying injury in the anteroposterior dimension display a sharp slope from ventral to dorsal in supine LPS-injured and Sph 1-P-treated cohorts, suggesting a gravitationally dependent predilection for lung edema formation in both groups (Figure 7). Furthermore, these vertical density gradients demonstrate increased air content in all lung regions in animals treated with intravenous Sph 1-P compared with those injured with LPS alone (Figure 7), with lung water accumulation most dramatic in gravitationally dependent, basilar lung. Sph 1-P dramatically attenuates the formation of alveolar edema with the most profound benefits observed in the transitional midlung regions (Figures 5–7).

## DISCUSSION

ALI represents a significant cause of morbidity and mortality in critically ill patients. Mechanical ventilation clearly contributes to the impact of the disease process through a variety of mechanisms, including direct mechanical injury to the alveolus

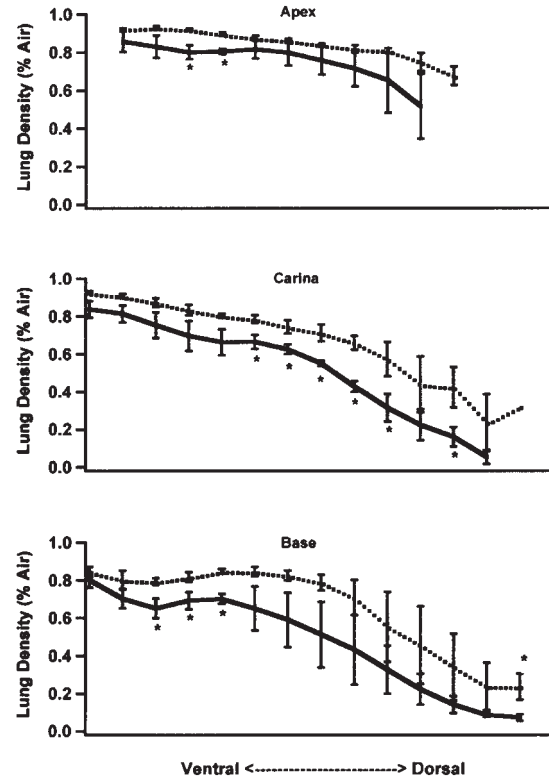


**Figure 7.** Intravenous Sph 1-P attenuates regional lung edema formation induced by intrabronchial LPS in a canine model of ventilator-associated lung injury. Depicted are vertical (anteroposterior) density gradients of beagles treated with intrabronchial LPS (2 mg/kg, solid,  $n = 3$ ) and beagles treated with intrabronchial LPS and concomitant intravenous Sph 1-P (85 mcg/kg, dotted,  $n = 3$ ). Vertical density gradients were generated segmenting the lung into apical (A), carina (B), and basilar (C) regions; 1-cm equal bins in the anteroposterior direction were generated, and the average density of each bin was measured. Sph 1-P improves aeration of transitional lung zones within each region with the most significant changes evident in the mid (carinal) lung region. Data represents mean  $\pm$  SEM. \* $p < 0.05$ .

and the alveolar capillary interface and through the generation of cytokines, which propagate the inflammatory process both locally within the lung and systemically (25–29). Treatment for ALI, however, remains largely supportive, without therapies that target specific pathogenetic mechanisms. Although ventilation strategies designed to limit mechanical injury to the alveolus improve outcomes from ALI (27, 30), adjunctive therapies to limit the duration of mechanical ventilation, such as surfactant administration or corticosteroid therapy, have not proven beneficial for treating adults with ALI to date (1, 3, 5). As a marked increase in vascular permeability with vascular leak into lung tissues is recognized as the central pathogenic cellular mechanism underlying the physiologic derangement characteristic of ALI, novel therapies that reduce lung microvascular permeability are likely to be clinically beneficial.

The lung endothelium is a functionally dynamic tissue that forms a semipermeable barrier between the vascular compartment and the parenchymal interstitium. Because of its enormous surface area, the lung vasculature is particularly sensitive to barrier dysregulation with increases in permeability. Disruption of the integrity of the endothelial cellular barrier occurs via ultrastructural changes characterized by cytoskeletal rearrangement and the generation of tensile forces within the cell resulting in cellular contrac-

tion, the interruption of intercellular adhesion complexes, and the creation of gaps between neighboring cells, which allow the exudation of fluid, macromolecules, and leukocytes into the interstitium and ultimately into the alveolar space, the pathological hallmark of ALI. Lung endothelial cell structure and function are greatly influenced by exposure to mechanical forces (31, 32), which can dramatically alter pulmonary vascular endothelial barrier properties. Cyclic stretch, greatly accentuated by mechanical ventilation, may invoke cytoskeletal rearrangement resulting in contraction of neighboring endothelial cell and disruption of intercellular adhesions, thus worsening endothelial barrier function and producing increased fluid flux across capillaries as demonstrated *in vitro* and in isolated perfused rat lung models (26, 31, 33). Similarly, the contractile apparatus is essential for agonist-induced changes in lung permeability, including those evoked by endotoxin (34, 35) and by thrombin, a regulatory molecule in the coagulation cascade (12).

We were the first to observe that Sph 1-P, a biologically active sphingolipid, enhances pulmonary vascular barrier function *in vitro* (12). Through signaling initiated by ligation of G-protein-coupled endothelial cell surface receptors, Sph 1-P induces cortical rearrangement of the cytoskeleton, stabilizing and enhancing intercellular and cell-matrix adhesion, which translates into improved barrier function as evidenced by increases in transmonolayer endothelial resistance (12). Recently, we demonstrated attenuation of inflammatory lung injury induced by intratracheal LPS in spontaneously ventilating C57BL/6 mice treated with parenteral administration of Sph 1-P or its structural analog FTY720 (13). In this study, we have extended these observations and demonstrated that intravenous Sph 1-P also attenuates the increased lung edema formation observed in a murine model of pure mechanical ventilation-induced lung injury, underscoring the importance of mechanical stress in this process. Mice treated with intravenous Sph 1-P 1 hour after exposure to high  $V_T$  mechanical ventilation displayed significant reductions in lung parenchyma Evans blue dye extravasation compared with vehicle-treated, mechanically ventilated mice (Figure 1).

Although rodent models may be used to establish the therapeutic potential of this approach, large animal experiments in injury models with appropriate scale and mechanical characteristics are essential to the translation of these therapies into the intensive care unit. Several large animal models of ALI have

been characterized in the literature, with oleic acid infusion, saline lung lavage, and acid aspiration representing those most commonly used. However, the injuries produced by these methods involve severe mechanical disruption of the endothelium or epithelium and, as such, may not be amenable to therapies that target endogenous barrier regulatory modalities. LPS challenge has been used to model clinical sepsis and pneumonia and, when combined with mechanical ventilation, results in significant lung injury. With intravenous administration, we observed profound hemodynamic compromise with limited lung injury despite elevated concentrations of endotoxin (data not shown). Intrabronchial endotoxin administration allowed us to focus the inflammatory reaction in the lung, producing a lung injury characterized by hypoxemia, increased shunt, reduced compliance, edema, and mechanical heterogeneity while maintaining hemodynamic stability (Table 1). In this clinically relevant canine model of LPS-induced ALI, we have demonstrated that Sph 1-P attenuates the oxygenation impairment induced by intrabronchial LPS instillation in part by interrupting the translocation of plasma proteins and water across the pulmonary microvascular endothelial barrier and into the alveolar airspace. Interestingly, although Sph 1-P was administered concurrent with the intrabronchial LPS, the improvement in oxygenation is delayed, requiring approximately 90 minutes before any physiologic effect becomes evident (Figure 2). After 90 minutes, the slopes of the venous admixture versus time curves diverge significantly ( $p < 0.05$ ), with an absolute improvement in shunt fraction evident 5.5 hours after injury induction. The mechanism of injury operative early in the time course remains unclear. It is possible that atelectasis occurs rapidly in both groups in response to LPS introduction, supported by the rapid increase in airway pressure in each group (Table 1). Despite hourly recruitment maneuvers, the acute inflammatory response and transient bronchoconstriction may make recruitment of these atelectatic regions difficult, resulting in ventilation/perfusion mismatch and shunting, which must recover before the barrier-enhancing effect of Sph 1-P becomes apparent. Although hydrostatic effects may contribute to the formation of alveolar edema in this model, this is likely minor, as the cardiac output, mean pulmonary artery pressure, and pulmonary artery occlusion pressure remain similar between groups (Table 1).

As demonstrated by CT imaging, mechanical heterogeneity is a fundamental property of ALI in humans, with different regions of the lung experiencing variable levels of collapse, flooding, cyclic

TABLE 1. GAS EXCHANGE, HEMODYNAMIC, AND AIRWAY MECHANICS PARAMETERS

	LPS			LPS + Sph 1-P		
	Baseline	90 min	6 h	Baseline	90 min	6 h
pH	7.39 ± 0.01	7.23 ± 0.01 <sup>†</sup>	7.20 ± 0.02 <sup>†</sup>	7.38 ± 0.02	7.21 ± 0.01 <sup>†</sup>	7.22 ± 0.01 <sup>†</sup>
Pa <sub>CO<sub>2</sub></sub> , mm Hg	35.6 ± 1.17	47.9 ± 1.56 <sup>†</sup>	42.8 ± 1.26 <sup>††</sup>	34.7 ± 1.47	46.3 ± 1.31 <sup>†</sup>	36.7 ± 1.26 <sup>§</sup>
Pa <sub>CO<sub>2</sub></sub> , mm Hg	145.9 ± 9.66	88.1 ± 4.28 <sup>†</sup>	78.9 ± 6.98 <sup>†§</sup>	145.9 ± 7.28	79.0 ± 6.39 <sup>†</sup>	83.3 ± 5.49 <sup>†</sup>
Pa <sub>CO<sub>2</sub></sub> /F <sub>IO<sub>2</sub></sub>	480.2 ± 31.6	243.9 ± 21.1 <sup>†</sup>	196.1 ± 19.0 <sup>†§</sup>	492.5 ± 24.4	233.5 ± 32.1 <sup>†</sup>	276.0 ± 24.2 <sup>†</sup>
MAP, mm Hg	102.1 ± 4.32	99.2 ± 3.32	105.9 ± 5.19	105.8 ± 5.58	102.3 ± 3.82	89.2 ± 7.99
CO, L/min	2.57 ± 0.25	2.52 ± 0.09	1.82 ± 0.23 <sup>††</sup>	2.80 ± 0.29	2.93 ± 0.98	1.79 ± 0.33 <sup>††</sup>
MPAP, mm Hg	14.5 ± 1.93	20.4 ± 1.50 <sup>†</sup>	21.9 ± 1.30 <sup>†</sup>	14.8 ± 1.10	18.1 ± 1.15 <sup>†</sup>	19.8 ± 0.65 <sup>†</sup>
PAOP, mm Hg	5.83 ± 0.57	7.67 ± 0.88	10.0 ± 0.70 <sup>†</sup>	5.63 ± 0.78	7.38 ± 1.24	10.4 ± 1.99 <sup>††</sup>
P <sub>plat</sub> , mm Hg	10.6 ± 0.85	14.4 ± 0.69 <sup>†</sup>	15.3 ± 0.42 <sup>†</sup>	10.9 ± 0.67	14.9 ± 1.01 <sup>†</sup>	15.3 ± 0.41 <sup>†</sup>
Hgb, g/dl	9.16 ± 0.39	9.9 ± 0.35	10.5 ± 0.45 <sup>†</sup>	9.77 ± 0.41	10.2 ± 0.48	10.4 ± 0.54
IVF, ml/kg/h*		24.9 ± 2.69			24.7 ± 3.56	

Definition of abbreviations: CO = cardiac output; Hgb = hemoglobin; IVF = intravenous fluid; LPS = lipopolysaccharide; MAP = mean arterial pressure; MPAP = mean pulmonary artery pressure; PAOP = pulmonary artery occlusion pressure; P<sub>plat</sub> = plateau airway pressure; Sph 1-P = sphingosine 1-phosphate.

\* Total intravenous fluid administration.

<sup>†</sup>  $p < 0.05$  compared with baseline.

<sup>††</sup>  $p < 0.05$  compared with 90 minutes.

<sup>§</sup>  $p < 0.05$  compared to LPS + Sph 1-P.

TABLE 2. PERIPHERAL BLOOD CELL PROFILES IN LIPOPOLYSACCHARIDE-INDUCED CANINE ALI

	WBC ( $\times 10^3$ )		ANC ( $\times 10^3$ )		ALC ( $\times 10^3$ )		Platelet ( $\times 10^3$ )	
	Baseline	5 h	Baseline	5 h	Baseline	5 h	Baseline	5 h
LPS	11.9 $\pm$ 7.7	3.4 $\pm$ 3.1*	8.5 $\pm$ 6.4	2.4 $\pm$ 2.7*	2.2 $\pm$ 0.9	0.8 $\pm$ 0.5*	239 $\pm$ 52	174 $\pm$ 59*
LPS + Sph 1-P	8.3 $\pm$ 3.3	1.7 $\pm$ 0.6*	5.9 $\pm$ 3.1	1.1 $\pm$ 0.4*	1.5 $\pm$ 0.7	0.7 $\pm$ 0.7*	216 $\pm$ 50	167 $\pm$ 35

Definition of abbreviations: ALC = absolute lymphocyte count; ANC = absolute neutrophil count; LPS = lipopolysaccharide; Sph 1-P = sphingosine 1-phosphate; WBC = white blood cell count.

\*p  $\leq$  0.05 compared with baseline.

stretch, and overdistension (14, 15, 19, 36). This heterogeneity is not captured in cellular or rodent models of ALI, which do not scale in terms of the effects of gravity, the interaction of the abdomen and chest wall, the mechanical interdependence of neighboring regions of the lung, or the hemodynamics and fluid dynamics. These factors further the need for large animal model validation of interventions successful in rodent models. For example, the likelihood that a particular intervention to limit lung injury in a mouse model will translate to patient care will depend on the degree that the mechanical conditions found in that model are represented in the heterogeneously injured human lung. Assuming a constant intrapulmonary blood volume, lung water accumulation is analogous to the change in lung tissue volume measured by CT imaging in the injured state compared with the normal condition.

Consistent with previous CT data from oleic acid and saline lavage injured dogs, lung water increased on the order of 1.7-fold after intrabronchial administration of LPS (Figure 4). Dramatically, intravenous Sph 1-P nearly completely prevented this increase in lung tissue volume (Figures 4 and 5). Furthermore, Sph 1-P reduced the accumulation of lung edema throughout the lung compared with LPS-injured animals, as demonstrated by the axial and vertical density profiles (Figures 6B and 7). The slight reduction in total lung volume (air plus tissue volumes, 794  $\pm$  119 vs. 899  $\pm$  24 ml, p = 0.2) observed in the LPS-treated animals is likely due to a combination of increased atelectasis and greater lung stiffness (lower air volume at same airway pressure), both of which reduce air volume and cannot be differentiated by this analysis. Absolute lung size may also contribute to this difference, although this is unlikely given the similar weights of the animals in each group (14.3  $\pm$  1.1-kg LPS vs. 14.6  $\pm$  0.8-kg Sph 1-P). Injury is most pronounced in the gravitationally dependent regions of all animals, whereas the nondependent apical regions are relatively spared (Figures 5–7). Sph 1-P improves aeration of lung at all levels in the vertical dimension, with the most significant improvements observed in the mid-dependent regions of the mid lung zone (Figure 7). The increased tissue density seen in the gravitationally dependent regions of the Sph 1-P-treated animals is likely the result of atelectasis in these regions rather than lung edema accumulation as the lung tissue volume in these dogs approaches that of historical control animals (Figure 4).

It is clear from the data presented that endothelial barrier enhancement with Sph 1-P attenuates edema formation in a rodent model of ventilator-induced lung injury as well as in a clinically relevant large animal model of ALI. Interestingly, the effect of Sph 1-P on lung edema accumulation is sustained despite the presumed short half-life of the compound *in vivo* because of rapid clearance from the circulation by sphingosine lyase (37, 38). In mice, the barrier-enhancing effect of Sph 1-P was sustained 24 hours after injection (13), and in the canine model, the vascular protective effect becomes evident approximately 2.5 hours after infusion and is sustained for at least 8 hours. The effects of Sph 1-P on alveolar edema formation in

intact animal models of ALI are likely due to multiple potentially synergistic mechanisms. Via ligation of cell surface receptors, Sph 1-P induces ultrastructural changes within the pulmonary microvascular endothelium, which manifest as barrier enhancement. These effects occur rapidly *in vitro* and are sustained for several hours (12). In addition to its endothelial cytoskeletal effects, Sph 1-P appears to modulate the immune response directly. With the exception of endothelial cells, Sph 1-P directly inhibits cellular motility of virtually all cell types (39, 40). Sph 1-P prevented neutrophil chemotaxis in response to IL-8 and the transmigration of neutrophils across an EC monolayer *in vitro* (41). We recently reported Sph 1-P-mediated decreases in neutrophil activity in lung and kidney tissues compared with mice treated with intratracheal LPS alone (13). Previous reports have suggested that Sph 1-P and several of its structural analogs decrease levels of circulating leukocytes (38). In this study, we observed leukopenia in beagles in response to intrabronchial LPS, an effect not altered by intravenous Sph 1-P (Table 2). Another potential effect of Sph-1-P may involve alterations in lung vascular vasoactivity with a recent study describing systemic vasorelaxation induced by nitric oxide released in response to endothelial differentiation gene-3 receptor ligation (42). Although this effect has not been studied in the pulmonary vasculature, temporary inactivation of the hypoxic pulmonary vasoconstrictive response via nitric oxide release could contribute to the increased shunt observed in the Sph 1-P-treated animals 90 minutes after injury induction (Figure 2) (43). This mechanism in isolation is unlikely, however, as restoration of hypoxic pulmonary vasoconstrictive alone would not lead to the decreased alveolar protein accumulation or the decreased lung edema observed. Finally, the effects of Sph 1-P on alveolar epithelial barrier function or on edema clearance mechanisms remain undefined at this point and represent a fertile area for future studies.

In summary, we have shown that Sph 1-P, a naturally occurring product of activated platelets and a potent *in vitro* barrier protective agonist, alters the course of ALI in a clinically relevant canine model through a variety of potential mechanisms, including decreasing endothelial permeability to fluid and macromolecules. This novel approach of pulmonary microvascular barrier modulation holds promise as a therapeutic strategy limiting the morbidity associated with prolonged mechanical ventilation in patients with ALI. Studies that address the efficacy of Sph 1-P administered as rescue therapy after well established ALI and in the presence of lung-protective low-Vt mechanical ventilation may further solidify the potential for this strategy in the care of the critically ill.

**Conflict of Interest Statement:** B.J.M. does not have a financial relationship with a commercial entity that has an interest in the subject of this manuscript; X.P. does not have a financial relationship with a commercial entity that has an interest in the subject of this manuscript; P.M.H. states that the results of this study do not impact on the past grant as the present shares; S.S. does not have a financial relationship with a commercial entity that has an interest in the subject of this manuscript; B.A.S. does not have a financial relationship with a commercial entity that has an interest in the subject of this manuscript; J.G.N.G. does not have a

financial relationship with a commercial entity that has an interest in the subject of this manuscript.

**Acknowledgment:** The authors gratefully acknowledge the expert technical assistance provided by Hilary Burman, Matthew Fuld, Diana Solana, and Philip Keller.

## References

- Anzueto A, Baughman RP, Guntupalli KK, Weg JG, Wiedemann HP, Raventos AA, Lemaire F, Long W, Zaccardelli DS, Pattishall EN. Aerosolized surfactant in adults with sepsis-induced acute respiratory distress syndrome: Exosurf Acute Respiratory Distress Syndrome Sepsis Study Group. *N Engl J Med* 1996;334:1417-1421.
- Anzueto A. Exogenous surfactant in acute respiratory distress syndrome: more is better. *Eur Respir J* 2002;19:787-789.
- Bernard GR, Luce JM, Sprung CL, Rinaldo JE, Tate RM, Sibbald WJ, Kariman K, Higgins S, Bradley R, Metz CA, et al. High-dose corticosteroids in patients with the adult respiratory distress syndrome. *N Engl J Med* 1987;317:1565-1570.
- Bernard GR, Vincent JL, Laterre PF, LaRosa SP, Dhainaut JF, Lopez-Rodriguez A, Steingrub JS, Garber GE, Helterbrand JD, Ely EW, et al. Efficacy and safety of recombinant human activated protein C for severe sepsis. *N Engl J Med* 2001;344:699-709.
- Gerlach H, Keh D, Semmerow A, Busch T, Lewandowski K, Pappert DM, Rossaint R, Falke KJ. Dose-response characteristics during long-term inhalation of nitric oxide in patients with severe acute respiratory distress syndrome: a prospective, randomized, controlled study. *Am J Respir Crit Care Med* 2003;167:1008-1015.
- Roy AJ, Djerassi I. Effects of platelet transfusions: plug formation and maintenance of vascular integrity. *Proc Soc Exp Biol Med* 1972;139:137-142.
- Gimbrone MA Jr, Aster RH, Cotran RS, Corkery J, Jandl JH, Folkman J. Preservation of vascular integrity in organs perfused in vitro with a platelet-rich medium. *Nature* 1969;221:33-36.
- Lo SK, Burhop KE, Kaplan JE, Malik AB. Role of platelets in maintenance of pulmonary vascular permeability to protein. *Am J Physiol* 1988;254:H763-H771.
- Shepro D, Welles SL, Hechtman HB. Vasoactive agonists prevent erythrocyte extravasation in thrombocytopenic hamsters. *Thromb Res* 1984;35:421-430.
- McDonagh PF. Platelets reduce coronary microvascular permeability to macromolecules. *Am J Physiol* 1986;251:H581-H587.
- Schaphorst KL, Chiang E, Jacobs KN, Zaiman A, Natarajan V, Wigley F, Garcia JGN. Role of sphingosine-1-phosphate in the enhancement of endothelial barrier integrity by platelet-released products. *Am J Physiol Lung Cell Mol Physiol* 2003;285:L258-L267.
- Garcia JG, Liu F, Verin AD, Birukova A, Dechert MA, Gerthoffer WT, Bamberg JR, English D. Sphingosine 1-phosphate promotes endothelial cell barrier integrity by Edg-dependent cytoskeletal rearrangement. *J Clin Invest* 2001;108:689-701.
- Peng X, Hassoun PM, Sammani S, Tuder RM, Burne-Taney MJ, Rabb H, McVerry BJ, Garcia JGN. Protective effects of sphingosine 1-phosphate in murine endotoxin-induced inflammatory lung injury. *Am J Respir Crit Care Med* 2004;169:1245-1251.
- Gattinoni L, Caironi P, Pelosi P, Goodman LR. What has computed tomography taught us about the acute respiratory distress syndrome? *Am J Respir Crit Care Med* 2001;164:1701-1711.
- Puybasset L, Cluzel P, Chao N, Slutsky AS, Coriat P, Rouby JJ. A computed tomography scan assessment of regional lung volume in acute lung injury: the CT Scan ARDS Study Group. *Am J Respir Crit Care Med* 1998;158:1644-1655.
- McVerry BJ, Simon BA, Garcia JGN. Sphingosine-1-phosphate attenuates endotoxin-induced lung injury in a canine model [abstract]. *Chest* 2003;124:181S.
- McVerry BJ, Simon BA, Garcia JGN. Sphingosine 1-phosphate reduces regional alveolar edema formation in a canine model of LPS-mediated acute lung injury [abstract]. *Am J Respir Crit Care Med* 2004;169:A708.
- Nunn J. Nunn's applied respiratory physiology. Oxford, MA: Butterworth-Heinemann; 1987. p. 165-168.
- Simon B. Non-invasive imaging of regional lung function using x-ray computed tomography. *J Clin Monit Comput* 2000;16:433-442.
- Simon B, Easley R, Baokye A. Regional differences in lung recruitment with PEEP after saline lavage. *Am J Respir Crit Care Med* 2001;163:A686.
- Simon B, Easley R. Regional recruitment is more uniform in prone versus supine position after oleic acid lung injury in dogs. *Am J Respir Crit Care Med* 2002;165:A682.
- Gattinoni L, Bombino M, Pelosi P, Lissoni A, Pesenti A, Fumagalli R, Tagliabue M. Lung structure and function in different stages of severe adult respiratory distress syndrome. *JAMA* 1994;271:1772-1779.
- Simon B, Marcucci C, Piper M, Downie J. CT P-V analysis differentiates flooding versus collapse in oleic acid and lavage injury models [abstract]. *Am J Respir Crit Care Med* 2000;161:A486.
- Downie JM, Nam AJ, Simon BA. Pressure-volume curve does not predict steady-state lung volume in canine lavage lung injury. *Am J Respir Crit Care Med* 2004;169:957-962.
- Webb HH, Tierney DF. Experimental pulmonary edema due to intermittent positive pressure ventilation with high inflation pressures: protection by positive end-expiratory pressure. *Am Rev Respir Dis* 1974;110:556-565.
- Parker JC. Inhibitors of myosin light chain kinase and phosphodiesterase reduce ventilator-induced lung injury. *J Appl Physiol* 2000;89:2241-2248.
- Ventilation with lower tidal volumes as compared with traditional tidal volumes for acute lung injury and the acute respiratory distress syndrome: the Acute Respiratory Distress Syndrome Network. *N Engl J Med* 2000;342:1301-1308.
- Imai Y, Parodo J, Kajikawa O, de Perrot M, Fischer S, Edwards V, Cutz E, Liu M, Keshavjee S, Martin TR, et al. Injurious mechanical ventilation and end-organ epithelial cell apoptosis and organ dysfunction in an experimental model of acute respiratory distress syndrome. *JAMA* 2003;289:2104-2112.
- Tremblay L, Valenza F, Ribeiro SP, Li J, Slutsky AS. Injurious ventilatory strategies increase cytokines and c-fos m-RNA expression in an isolated rat lung model. *J Clin Invest* 1997;99:944-952.
- Amato MB, Barbas CS, Medeiros DM, Magaldi RB, Schettino GP, Lorenzi-Filho G, Kairalla RA, Deheinzelin D, Munoz C, Oliveira R, et al. Effect of a protective-ventilation strategy on mortality in the acute respiratory distress syndrome. *N Engl J Med* 1998;338:347-354.
- Birukov KG, Jacobson JR, Flores AA, Ye SQ, Birukova AA, Verin AD, Garcia JGN. Magnitude-dependent regulation of pulmonary endothelial cell barrier function by cyclic stretch. *Am J Physiol Lung Cell Mol Physiol* 2003;00336:2002.
- Birukov KG, Birukova AA, Dudek SM, Verin AD, Crow MT, Zhan X, DePaola N, Garcia JG. Shear stress-mediated cytoskeletal remodeling and cortactin translocation in pulmonary endothelial cells. *Am J Respir Cell Mol Biol* 2002;26:453-464.
- Parker JC, Hernandez LA, Peevy KJ. Mechanisms of ventilator-induced lung injury. *Crit Care Med* 1993;21:131-143.
- Bannerman DD, Goldblum SE. Endotoxin induces endothelial barrier dysfunction through protein tyrosine phosphorylation. *Am J Physiol* 1997;273:L217-L226.
- Bannerman DD, Goldblum SE. Direct effects of endotoxin on the endothelium: barrier function and injury. *Lab Invest* 1999;79:1181-1199.
- Gattinoni L, Presenti A, Torresin A, Baglioni S, Rivolta M, Rossi F, Scarani F, Marcolin R, Cappelletti G. Adult respiratory distress syndrome profiles by computed tomography. *J Thorac Imaging* 1986;1:25-30.
- Pyne S, Pyne N. Sphingosine 1-phosphate signalling via the endothelial differentiation gene family of G-protein-coupled receptors. *Pharmacol Ther* 2000;88:115-131.
- Mandala S, Hajdu R, Bergstrom J, Quackenbush E, Xie J, Milligan J, Thornton R, Shei GJ, Card D, Keohane C, et al. Alteration of lymphocyte trafficking by sphingosine-1-phosphate receptor agonists. *Science* 2002;296:346-349.
- Panetti TS. Differential effects of sphingosine 1-phosphate and lysophosphatidic acid on endothelial cells. *Biochim Biophys Acta* 2002;1582:190-196.
- Liu F, Verin AD, Wang P, Day R, Wersto RP, Chrest FJ, English DK, Garcia JG. Differential regulation of sphingosine-1-phosphate- and VEGF-induced endothelial cell chemotaxis: involvement of G(ialpha2)-linked Rho kinase activity. *Am J Respir Cell Mol Biol* 2001;24:711-719.
- Kawa S, Kimura S, Hakomori S, Igarashi Y. Inhibition of chemotactic motility and trans-endothelial migration of human neutrophils by sphingosine 1-phosphate. *FEBS Lett* 1997;420:196-200.
- Nofer JR, van der Giet M, Tolle M, Wolinska I, von Wnuck Lipinski K, Baba HA, Tietge UJ, Godecke A, Ishii I, Kleuser B, et al. HDL induces NO-dependent vasorelaxation via the lysophospholipid receptor S1P3. *J Clin Invest* 2004;113:569-581.
- Schuster DP, Kozlowski JK, McCarthy T, Morrow J, Stephenson A. Effect of endotoxin on oleic acid lung injury does not depend on priming. *J Appl Physiol* 2001;91:2047-2054.